

# Chapter 4

## H I Column Density Statistics of the Cold Neutral Medium from Absorption Studies<sup>1</sup>

### 4.1 Introduction

The structure, physical condition, and dynamical evolution of an ISM is significantly affected by the turbulence within it (Scalo and Elmegreen, 2004). Turbulence produces scale-invariant structures in the density and velocity fluctuations of H I in ISM. In Lazarian and Pogosyan (2000), Lazarian and Pogosyan (2004), and Dutta (2016) different methods have been proposed (and used) to study these types of fluctuations. Large scale ( $\sim$  few kpcs) structures of the H I are studied with the help of H I-21 cm emission and results for some external spiral galaxies are presented in Elmegreen et al. (2001), Dutta and Bharadwaj (2013). On the other hand, studies of the Galactic structures over few parsecs are published in Crovisier and Dickey (1983) and Green (1993). The small scale structures of H I are

---

<sup>1</sup>The work presented in this chapter is derived from the original work published as "H I Column Density Statistics of the Cold Neutral Medium from Absorption Studies" by Vishwakarma and Dutta (2019).

probed with the help of the 21-cm absorption studies against the bright background sources, helping us to probe the cold neutral medium (CNM) phase of the ISM. At scales of few parsecs and lower, the studies by Faison and Goss (2001) and Brogan et al. (2005) have shown that there exist scale-invariant structures along a few line of sight in the Galaxy (see also Stanimirović and Zweibel (2018)). In a study, where using the fast-moving pulsars as a background source, Galactic optical depth variation along few line of sight at the scales of 5-100 au have been observed (Frail et al., 1994), on the other hand, another study by Johnston et al. (2003) and Stanimirović et al. (2003) have not shown any significant variation in the optical depth (Galactic) along few other lines of sight. Another interesting way to study the CNM structures is: measuring the two-point correlation function of optical depth against extended background sources like supernovae remnants or radio galaxies (Deshpande et al., 2000; Dutta et al., 2014; Roy et al., 2010). It is still unclear whether these observed small-scale fluctuations represent some physical process or they are just transient structures observed at a particular line of sight in our Galaxy (Deshpande, 2000). The existence of the coherent, small scale structures signifies the change in the star formation activity (Krumholz, 2014); on the other hand, if these small scale structures are just short-lived entities, then their study may shed light on the unstable phase of the ISM. In this chapter, we study the statistics of the CNM phase of the Galactic ISM by measuring the two-point correlation function of the opacity (optical depth) fluctuations. In section 2, we present the visibility based method to calculate the two-point statistics (correlation function) of optical depth while its relation with column density and spin temperature statistics is analyzed in section 3. In section 4, we observe the effect of CNM physical parameters and observables on such an estimator, followed by the discussion and conclusion of this chapter in section 5.

	Auto-correlation	Power spectrum
Continuum	$\xi_{I_c}(\vec{\theta})$	$P_{I_c}(\vec{U})$
Line	$\xi_I(\vec{\theta}, \nu)$	$P_I(\vec{U}, \nu)$
Optical depth	$\xi_\tau(\vec{\theta}, \nu)$	$\Xi(\vec{U}, \nu)$

Table 4.1 Different auto-correlation functions and the corresponding power spectrum of the observables used in this chapter.

## 4.2 Two point statistics of the optical depth from observed visibilities

### 4.2.1 Specific intensity of 21-cm radiation

The simple solution for the radiative transfer equation towards an extended background source can be written as (see Draine (2011)),

$$I(\vec{\theta}, \nu) = I_c(\vec{\theta})e^{-\tau(\vec{\theta}, \nu)}, \quad (4.1)$$

here  $I(\vec{\theta}, \nu)$  represents the specific intensity in the direction of the background source,  $I_c(\vec{\theta})$  is the continuum part of the radiation in the same direction,  $\tau(\vec{\theta}, \nu)$  is the optical depth of the intervening cloud in the same direction and  $\vec{\theta}$  represents the direction in sky relative to center of field of view. We consider  $I_c(\vec{\theta})$  not being a function of frequency, and model it as mean added by fluctuating component of it over its mean i.e.

$$I_c(\vec{\theta}) = W(\vec{\theta})[\bar{I}_c + \Delta I_c(\vec{\theta})], \quad (4.2)$$

Here  $\bar{I}_c$  is the total continuum flux of the background source while  $W(\vec{\theta})$  is the window function following the property  $\int d\vec{\theta} W(\vec{\theta}) = 1$ .  $\Delta I_c(\vec{\theta})$  represents zero mean small scale

fluctuations of the continuum. Similar to the  $I_c(\vec{\theta})$ , we also model  $\tau(\vec{\theta}, \nu)$  as

$$\tau(\vec{\theta}, \nu) = \bar{\tau}(\nu) + \Delta\tau(\vec{\theta}, \nu), \quad (4.3)$$

where  $\bar{\tau}(\nu)$  is the average (spatially) optical depth in the given frequency  $\nu$  and  $\Delta\tau(\vec{\theta}, \nu)$  is the fluctuating component of the optical depth over mean. From the above equations,  $I(\vec{\theta}, \nu)$  in the form of above models can be written as

$$I(\vec{\theta}, \nu) = W(\vec{\theta}) \left[ \bar{I}_c + \Delta I_c(\vec{\theta}) \right] e^{-[\bar{\tau}(\nu) + \Delta\tau(\vec{\theta}, \nu)]} \quad (4.4)$$

### 4.2.2 Autocorrelation function of optical depth fluctuations

If we represent the auto-correlation function of the  $I(\vec{\theta}, \nu)$  by  $\xi_I(\vec{\theta}, \vec{\theta}', \nu)$ , then it can be defined as

$$\xi_I(\vec{\theta}, \vec{\theta}', \nu) = \langle I(\vec{\theta}, \nu) I(\vec{\theta}', \nu) \rangle, \quad (4.5)$$

Here  $\langle \rangle$  stands for the ensemble averaging. Similarly the auto-correlation of the  $I_c(\vec{\theta})$  also can be written as  $\xi_{I_c}(\vec{\theta}, \vec{\theta}') = \langle I_c(\vec{\theta}) I_c(\vec{\theta}') \rangle$ . Following the Roy et al. (2010), the auto-correlation of the  $I(\vec{\theta}, \nu)$  in term of the optical depth parameters ( $\bar{\tau}(\nu)$  and  $\sigma_\tau(\nu)$ ) and  $\xi_{I_c}(\vec{\theta}, \vec{\theta}')$  can be written as

$$\xi_I(\vec{\theta}, \nu) = e^{-2\bar{\tau}(\nu) + \sigma_\tau^2(\nu)} \xi_{I_c}(\vec{\theta}) e^{\xi \tau(\vec{\theta}, \nu)}, \quad (4.6)$$

Here  $\sigma_\tau(\nu)$  is the standard deviation of  $\tau(\vec{\theta}, \nu)$ , measured over the angular directions  $\vec{\theta}$ .  $\xi_\tau$  represents the two point correlation function of optical depth and can be written as

$$\xi_\tau(\vec{\theta}, \nu) = \langle \Delta\tau(\vec{\theta}, \nu) \Delta\tau(\vec{\theta}', \nu) \rangle. \quad (4.7)$$

Here  $\xi$  is used to represent the two point correlations of the different estimators and are listed in table 4.1.

### 4.2.3 Measuring the optical depth autocorrelation from radio-interferometric observations

Radio-interferometers measure the Fourier transform of the sky brightness distribution in the form of visibilities  $V(\vec{U}, \nu)$  (Thompson et al., 2017) as

$$V(\vec{U}, \nu) = \int A(\vec{\theta})W(\vec{\theta})I(\vec{\theta}, \nu)e^{-2\pi i\vec{U}\cdot\vec{\theta}}d\vec{\theta}, \quad (4.8)$$

Here  $A(\vec{\theta})$  is the reception pattern of the antenna. To represent the visibility correlation in the line channel we use the term  $V_2(\vec{U}, \vec{U}', \nu)$  defined as

$$V_2(\vec{U}, \vec{U}', \nu) = |\tilde{W}(\vec{U})|^2 \otimes [\delta_{2D}(\vec{U} - \vec{U}')P_I(\vec{U}, \nu)], \quad (4.9)$$

Here  $\otimes$  stands for the convolution symbol and  $\Delta_{2D}$  is the 2-dimensional Dirac delta function. The quantity  $P_I(\vec{U}, \nu)$  represents the power spectrum of  $I_\nu$  (specific intensity), and it is the Fourier transform of  $\xi_I(\theta, \nu)$  i.e.

$$P_I(\vec{U}, \nu) = \int \xi_I(\vec{\theta}, \nu) e^{-2\pi i\vec{U}\cdot\vec{\theta}}d\vec{\theta} \quad (4.10)$$

where  $\tilde{W}(\vec{U}) = \int A(\vec{\theta})W(\vec{\theta})e^{-2\pi i\vec{U}\cdot\vec{\theta}}d\vec{\theta}$ . For the interferometers like GMRT, VLA whose field of view is  $\geq 45'$  at 1420 MHz,  $\tilde{W}(\vec{U})$  dominates, as our chosen background sources have maximum size  $\sim 10'$ . If we represent the correlation of the continuum visibilities

as  $V_{2c}(\vec{U}, \vec{U}')$ , then the visibility correlation in the line (H I absorption) channel can be written as

$$V_2(\vec{U}, \vec{U}', \nu) = e^{-2\bar{\tau}(\nu) + \sigma_{\bar{\tau}}^2(\nu)} V_{2c}(\vec{U}, \vec{U}') \otimes \Xi(\vec{U}, \nu), \quad (4.11)$$

Here term  $\Xi(\vec{U}, \nu)$  keeps the statistical information of  $\xi_{\tau}(\vec{\theta}, \nu)$  and defined as

$$\Xi(U, \nu) = \int d\theta e^{\xi_{\tau}(\vec{\theta}, \nu)} e^{-2\pi i \vec{U} \cdot \vec{\theta}}. \quad (4.12)$$

In this work, we focus on the structure of the CNM phase of the ISM at the length scales of subparsec to few tens of parsec. Our work presented here is limited up to isotropic fluctuation consideration (i.e.  $\vec{U} = |U|$ ) rather than anisotropic considerations as discussed by (Martin et al., 2015), Kalberla et al. (2017), Blagrove et al. (2017), Clark et al. (2019) for the Galactic structures seen over the length scales of  $\sim$  pc to few hundreds of pc.

### 4.3 Relation of optical depth autocorrelation with statistics of the H I column density and spin temperature

The 21-cm optical depth as a function of  $\vec{\theta}$  and  $\nu$  is given as (see Draine (2011))

$$\tau(\vec{\theta}, \nu) = \frac{3hc^2 A_{21}}{32\pi k_B \nu_0} \int dz \frac{n_{HI}(\vec{\theta}, z)}{T_s(\vec{\theta}, z)} \phi(\vec{\theta}, z, \nu), \quad (4.13)$$

Here  $\nu_0$ ,  $k_B$  and  $A_{21}$  are the rest frequency (21-cm), Boltzmann constant and Einstein's A coefficient respectively. In the above equation  $z$ ,  $n_{HI}$  and  $T_s$  represent the line of sight direction, H I number density and spin temperature of the medium respectively.  $\phi$  in the above equation represents the line shape function and follow the property  $\int \phi(\nu) d\nu = 1$ . Here we have assumed that  $\phi$  is independent of the sky direction (i.e. lines of sight) and can be treated as a constant at the frequency of our interest. We model  $n_{HI}$  and  $T_s$  of the

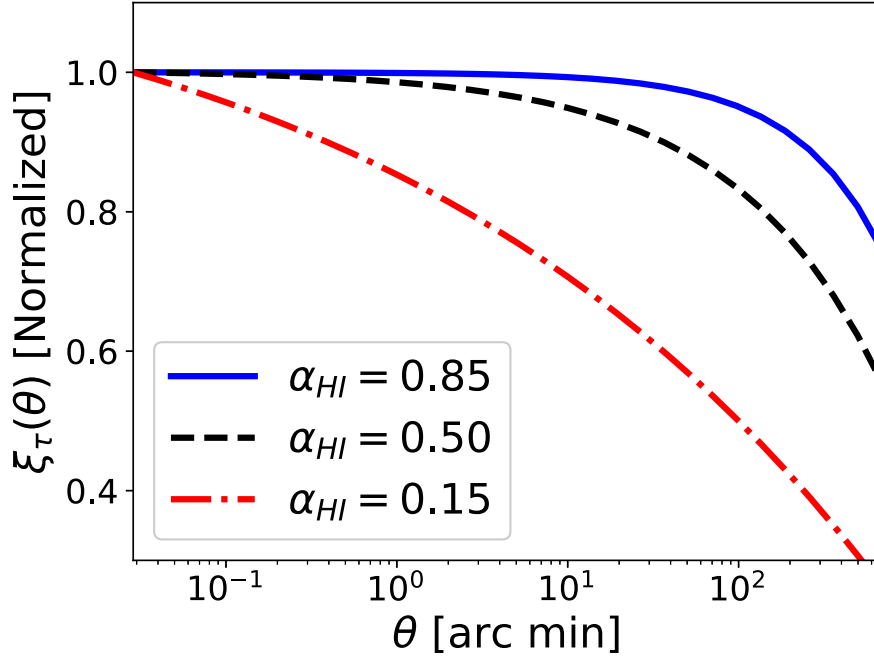


Fig. 4.1 : Variation of optical depth auto-correlation function  $\xi_\tau(\theta)$  as a function of  $\theta$  for different values of  $\alpha_{HI}$ . Here  $\gamma$ ,  $\eta$  and  $\sigma_{HI}$  are taken 0, 0.5 and 0.1 respectively.

optical depth as mean (represented by "-") and fluctuating component of it over mean as

$$\begin{aligned} n_{HI}(\vec{\theta}, z) &= \bar{n}_{HI} \left[ 1 + \delta_{n_{HI}}(\vec{\theta}, z) \right] \\ T_s(\vec{\theta}, z) &= \bar{T}_s \left[ 1 + \delta_{T_s}(\vec{\theta}, z) \right]. \end{aligned} \quad (4.14)$$

If we assume the above fluctuations to be small in comparison to 1, then using expansion only up to first-order,  $\tau(\vec{\theta}, \nu)$  can be written as

$$\tau(\vec{\theta}, \nu) = \bar{\tau}(\nu) \int \frac{dz}{L} \left[ 1 + \delta n_{HI}(\vec{\theta}, z) - \delta T_s(\vec{\theta}, z) \right], \quad (4.15)$$

where  $\bar{\tau}(\nu) = \frac{3hc^2 A_{21}}{32\pi k_B \nu_0} \frac{\bar{N}_{HI}}{T_s} \phi(\nu)$ . In the above equation L, represent the characteristic length scale of the cloud along the line of sight and  $\bar{N}_{HI} = \int dz \bar{n}_{HI}$  is the average (spacially) column density. Henceforth, we shall consider all relevant quantities for a single frequency and not use " $\nu$ " explicitly.

From equations 4.3 and 4.13, we find that

$$\Delta\tau(\vec{\theta}) = \frac{\bar{\tau}}{L} \int dz \left[ \delta n_{HI}(\vec{\theta}, z) - \delta T_s(\vec{\theta}, z) \right], \quad (4.16)$$

We assume the fluctuations in number density  $n_{HI}$  and spin temperature  $T_s$  are homogeneous and isotropic. Correlating the optical depth fluctuations  $\Delta\tau(\vec{\theta})$  at two different  $\vec{\theta}$  we get

$$\xi_\tau(\theta) = \frac{\bar{\tau}^2}{L} \int dz [\zeta_{HI}(\theta, z) + \zeta_{T_s}(\theta, z) - 2\zeta_{HT}(\theta, z)], \quad (4.17)$$

where the cross-correlations and autocorrelations  $\zeta$  are defined as

$$\zeta_{ab}(\theta, z) = \langle \delta a(\vec{\theta}_1, z_1) \delta b(\vec{\theta}_2', z_2') \rangle. \quad (4.18)$$

Here  $\theta = |\theta_1 - \theta_2|$  and  $z = |z_1 - z_2|$  gives the separation between the two points along which the correlation is calculated. Since the fluctuations are assumed to be homogeneous and isotropic the quantity  $\xi_\tau$  does not depend on the location and direction of the separation vector between the two points where the correlations  $\zeta_{ab}$  are calculated. The physical conditions of the CNM cloud that may exist in the ISM are, (1) CNM clouds may be in both pressure and thermal equilibrium; in this case,  $\delta T_s = -\delta n_{HI}$  will be followed i.e. fluctuations in the column density and spin temperature will be correlated, (2) It is also possible that CNM clouds being in thermal equilibrium behaves like adiabatic gas with  $\gamma = 5/3$ . In such a condition,  $\delta T_s = -\delta n_{HI}(1 - \gamma)$  will be followed where  $\gamma$  being the adiabatic gas index, 3) In spite of the above possibilities, it is also possible that, in CNM  $n_{HI}$  and  $T_s$  may not be correlated at all. In general a combination of correlated and uncorrelated gas may co-exist, i.e,  $\delta T_s = -\eta(1 - \gamma) \delta n_{HI} + (1 - \eta) \times \text{uncorrelated part}$ . Here  $\eta$  represents the fractional correlation. Hence we get,

$$\xi_\tau(\theta) = \bar{\tau}^2 \left[ \chi \xi_{HI}(\theta) + (1 - \eta)^2 \sigma_{T_s^2} \right], \quad (4.19)$$



where  $\chi = [1 + \eta(1 - \gamma)]^2$  and  $\xi_{HI}(\theta)$  is defined as  $\xi_{HI}(\theta) = \frac{1}{L} \int dz \zeta_{HI}(\theta, z)$ . At  $\theta = 0$ , above equation reduces to the variance of  $\tau$  and can be written as

$$\sigma_{\tau}^2 = \bar{\tau}^2 \left[ \chi \sigma_{HI}^2 + (1 - \eta)^2 \sigma_{T_s^2} \right]. \quad (4.20)$$

Using the definition of  $\sigma_{T_s^2}$  from equation (4.20 in 4.20) we get

$$\xi_{\tau}(\theta) = \sigma_{\tau}^2 - \chi \bar{\tau}^2 \sigma_{HI}^2 \theta^{\alpha_{HI}}. \quad (4.21)$$

Here we assume that the 2-dimensional power spectrum  $P_{HI}(U)$  of the H I column density fluctuation is a power law with power law index  $-(2 + \alpha_{HI})$ , i.e,  $P(U) \propto U^{-(2 + \alpha_{HI})}$ . The quantities  $\tau$  and  $\sigma_{\tau}$  can be calculated from the optical depth map ( see Dutta et al. (2014) and Dutta and Nandakumar (2019)). Hence the function  $\Xi(\vec{U})$  posses information about  $\alpha_{HI}$ ,  $\gamma$ ,  $\eta$  and  $\sigma_{HI}$ . It is also clear from equation 4.21 that  $\eta$ ,  $\gamma$  and  $\sigma_{HI}$  are degenerate if we have only  $\xi_{\tau}(\theta)$  as a measure.

## 4.4 Sensitivity of observables on the physical parameters

### 4.4.1 With isotropic column density fluctuations

Here we discuss how  $\Xi(\vec{U})$  is sensitive and dependent on the physical parameters  $\alpha_{HI}$ ,  $\gamma$ ,  $\eta$  and  $\sigma_{HI}$ , under the assumption that H I column density fluctuation is isotropic. As discussed earlier that  $\tau$  and  $\sigma_{\tau}$  can be estimated from the observational measure of the optical depth map. It also has been shown that at  $\tau = 1$ , bias in the measurements of  $\tau$  and  $\sigma_{\tau}$  is minimum (Dutta et al., 2014), so we will use the fiducial values of these as 1 and 0.1 respectively. The unbiased and scale independent correlation function of the optical depth can be accessed using the visibility based correlation method and here we use the same. The two fiducial values of  $\gamma$  chosen here are 0 and 5/3.  $\gamma = 0$  corresponds

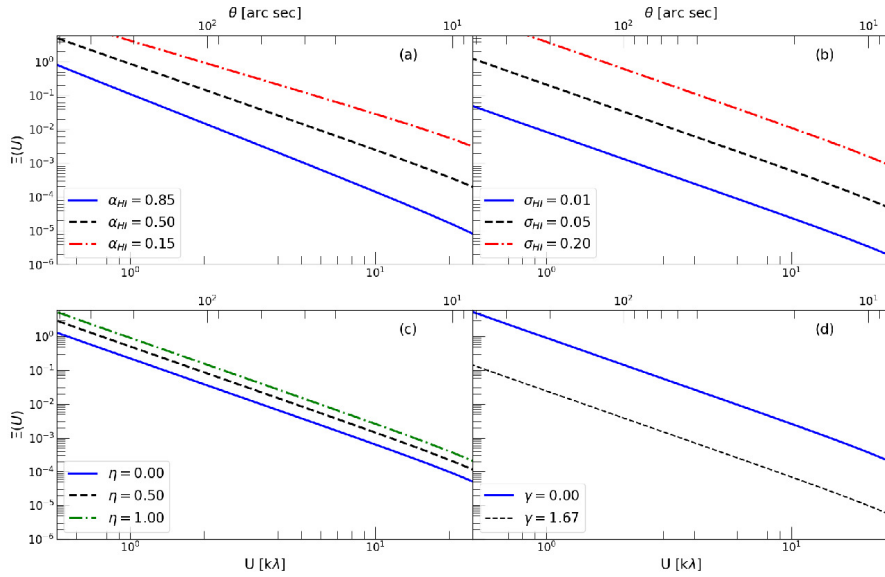


Fig. 4.2 : Variation of  $\Xi(\vec{U})$  with baselines ( $U$ ) is shown for different values of the parameters  $\alpha_{HI}$ ,  $\sigma_{HI}$ ,  $\eta$  and  $\gamma$ . In each panel, one of the parameters is varied, keeping the other fixed (see section 4 of this chapter).

to  $\chi = 1$  if  $\eta = 0$  and it ( $\chi$ ) have maximum value if  $\eta = 1$ . For  $\gamma = 5/3$ , the variation of  $\chi$  is rather slow for the values of  $\eta$  between 0 and 1. We take the values of  $\eta$  as [0, 0.5, 1] to observe its effect on  $\Xi(\vec{U})$ , here  $\eta = 0.5$  will be chosen as its fiducial value. We choose the values of  $\sigma_{HI} = [0.01, 0.05, 0.20]$ , as study of the structures at large scales through H I emission have shown that H I fluctuations are generally  $\sim 10\%$  over the mean (Dutta and Bharadwaj, 2013). So, 0.1 is chosen as the fiducial value of the  $\sigma_{HI}$ . The study of the optical depth fluctuation in the direction of Cassiopeia-A have shown that  $\sigma_\tau = 2(x/4pc)^{0.34}$ , corresponding to the 0.68 for  $\alpha_{HI}$ , so we choose the values of  $\alpha_{HI}$  as [0.15, 0.5, 0.85] where 0.5 will be used as fiducial value for  $\alpha_{HI}$ . In figure 4.1, we show the two-point correlation function of the optical depth in the normalized form (equation 4.21), for the values of the  $\alpha_{HI} = [0.15, 0.5, 0.85]$ . The values of the other physical parameters in the plots were taken as 0, 0.05 and 0.1 (for  $\gamma$ ,  $\eta$  and  $\sigma_{HI}$  respectively). In figure 4.2, we show the variation of  $\Xi(\vec{U})$  as a function of these parameters in the baseline range (0.5-20kλ). In figure 4.2(a) we show  $\Xi(\vec{U})$ , where it assumes the power-law having index

of  $[-2.85, -2.5, -2.15]$  for the values of  $\alpha_{HI}$   $[0.85, 0.5, 0.15]$  respectively. For the small scale fluctuations (over mean) in the optical depth,  $\Xi(\vec{U})$  is expected to show the same functional form as the power spectrum of the optical depth i.e. slope of  $\Xi(\vec{U})$  in log-log scale should be  $-2-\alpha_{HI}$  (Lee and Jokipii, 1975). This demonstrates that the power law index of the scale-invariant fluctuations in the column density of H I can be estimated directly from opacity scale invariant fluctuation. From the other three subfigures of the figure number 4.2, it can be seen that amplitude of the  $\Xi(\vec{U})$  is dependent on the other three parameters  $\gamma$ ,  $\eta$ , and  $\sigma_{HI}$  while the slope is independent of these. Here amplitude of  $\Xi(\vec{U})$  is found to be  $\propto \sigma_{HI}^2$  as expected for small scale fluctuations. In figure 4.2(b) we show variation of  $\Xi(\vec{U})$  for three different values of  $\sigma_{HI}$  while fixing other parameters ( $\gamma = 0$ ). In figure 4.2(c), we fix all other parameters by their fiducial values and show the variation of  $\Xi(\vec{U})$  with  $\eta$ , and finally, the variation of  $\Xi(\vec{U})$  with  $\gamma$  is shown in figure 4.2(d), keeping all other parameters fixed. All of the above discussions it is clear that, to measure any one of the above three physical parameters ( $\sigma_{HI}$ ,  $\eta$  and  $\gamma$ ) other two must be known as only optical depth observation will not suffice for such an intended measurement.

#### 4.4.2 Effect of anisotropic fluctuations

In the previous section, we accessed the isotropic estimator of the H I column density fluctuation with the help of optical depth fluctuations. In work by Goldreich and Sridhar (1995), the magnetized part of ISM has been modeled to have anisotropic fluctuations. In such a case, turbulence is expected to show scale-independent structures with anisotropic characteristics governed by Alfvén Mach number (Burkhart et al., 2014; Esquivel and Lazarian, 2011). In the recent efforts, it has been worked out to define the anisotropic structures of the ISM with the help of the multipole moments incorporated in the structure-function (Kandel et al., 2017). Observations of the anisotropic structures in the Magellanic bridge and Galaxy (associated with H I distribution) also have been studied and are

presented in Muller et al. (2004), Kalberla and Kerp (2016) and Kalberla et al. (2017). The above studies concluded that the anisotropic structures associated with H I distribution are almost scale independent. They use the ratio  $Q = P(U, \phi = 0)/P(U, \phi = \pi/2)$  to define the power associated with anisotropy where azimuthal angle  $\phi$ . Where  $\phi = 0$  corresponds to the direction of maximum power. We here study that how in the anisotropic case, the amplitude of our isotropic estimator  $\Xi(\vec{U})$  (or power spectra) scales. We model the scale-independent power spectra associated with anisotropic optical depth at 21 cm as

$$P_{\tau}(U, \phi) = A \Phi(\phi) U^{-2-\alpha_{HI}}, \text{ where} \quad (4.22)$$

$$\Phi(\phi) = \left[ \frac{f_a \cos^2 \phi + 1}{f_a + 1} \right].$$

Here  $\phi$  is the azimuthal angle as introduced earlier in this section. In this model, slope  $-2 - \alpha_{HI}$  of the spectra remains same as for the isotropic case, while amplitude  $A$  carries information about anisotropic power through function  $\Phi(\phi)$ . Here  $f_a$  in  $\Phi(\phi)$  represents the anisotropy parameter. In the literature  $f_a$  is related to  $Q$  as  $Q = f_a + 1$  i.e.  $f_a = 0 (Q = 1)$  is equivalent to the isotropic fluctuation. In figure 4.3 we show the variation of  $\Phi(\phi)$  with  $\phi$  for different  $f_a$ . If we use  $P(U)$  as a representative of the isotropic power spectrum for the optical depth fluctuations then

$$P(U) = \frac{1}{2\pi} \int_0^{2\pi} P(U, \phi) d\phi \quad (4.23)$$

$$= A \mathcal{R}(f_a) U^{-2-\alpha_{HI}}, \text{ where}$$

$$\mathcal{R}(f_a) = \frac{f_a + 2}{2(f_a + 1)}.$$

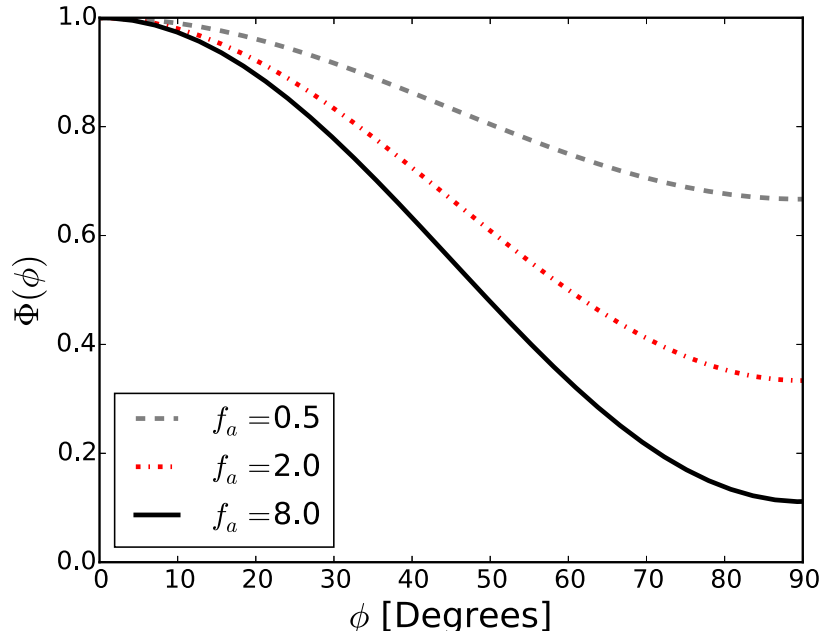


Fig. 4.3 : Variation of  $\Phi$  as a function of azimuthal angle  $\phi$  in the baseline plane for different values of the anisotropy parameter  $f_a$ .

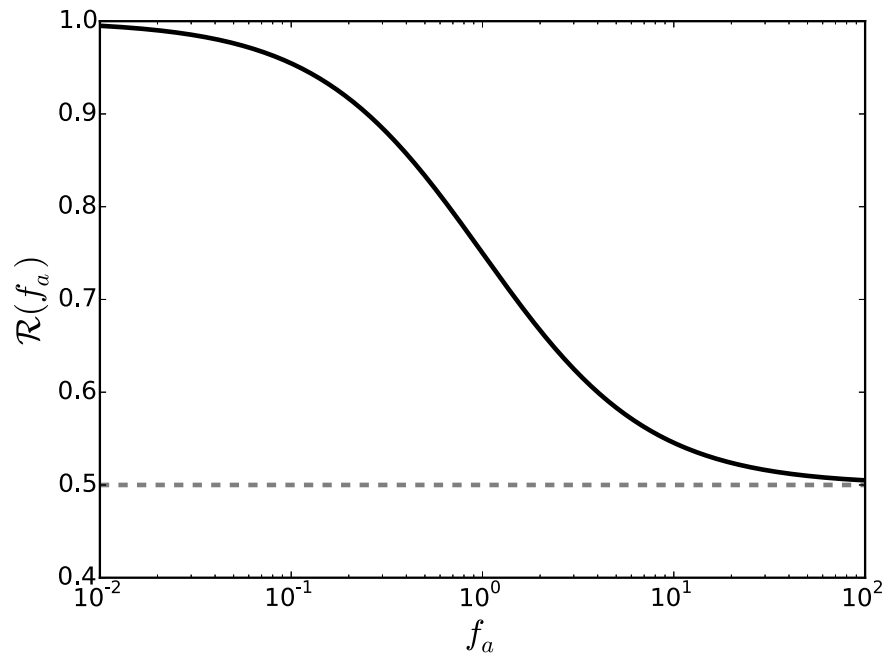


Fig. 4.4 : Variation of  $\mathcal{R}$  with anisotropy parameter  $f_a$ . The asymptotic value of  $\mathcal{R}$  (0.5) is represented by dashed gray line.

We find that only the amplitude scaling (through  $\mathcal{R}(f_a)$ ) of the isotropic power spectrum takes place if we want to use it to describe an anisotropic (scale independent) scale-invariant H I structure. The thing which has to be noted here is that the scaling depends upon our considered model  $\Phi(\phi)$ . In figure 4.4 we show the variation of  $\mathcal{R}(f_a)$  with  $f_a$  for our considered model. In this model, for large value of  $f_a$ , the anisotropic power  $R(f_a)$  approaches  $1/2$ .

## 4.5 Discussion and Conclusion

In this chapter, we studied the possible physical conditions of the CNM and further discussed the possibility of estimating the physical parameters associated with the CNM with the help of the optical depth autocorrelation function. The scale-invariant fluctuations of the H I column density in the ISM is expected to be the result of the compressible fluid turbulence. Our results found that only measurements of the statistics of the optical depth fluctuations do not suffice to trace much about its amplitude and dependence on the physical parameters. The amplitude of the optical depth autocorrelation function has the same behavior, whether spin temperature and column density in the CNM are correlated to each other or not (or even partially correlated). However, a multiwavelength study like Wakker et al. (2011) at the same line of sight may shed more light on such a study; on the other hand, different spectral line observations (along the same line of sight) may help to study the spin temperature fluctuations too, if the condition of thermal equilibrium hold. The main outcome that we found from the studies in this chapter follows that H I column density fluctuation can be studied with the help of the radio interferometric observations of the optical depth fluctuations at the subparsec scales.

Numerical simulations study of the specific intensity of  $^{13}\text{CO}$  by Burkhart et al. (2014) has shown that the power-law index of the specific intensity fluctuations for the optically thick medium saturates at  $-3.0$ , same as expected by Lazarian and Pogosyan (2004). For

such a study, the index for the optically thin medium is expected to be shallower. Recently Bournaud et al. (2010) studied the Galactic ISM using simulations, where he found that gas surface density to have power-law index  $-2.8$  to  $-3.0$  at the large scales (100 pc or lower), depending upon the Galactic dynamics. A similar study by Grisdale et al. (2016) found that galaxies of the Milky-Way size show a power spectrum of H I column density of power-law index  $-2.5$ , when stellar feedback effect consideration is taken into account. The H I structures at the scales of pc and higher are studied with the help of the H I emission observations, from where the power spectrum of H I column density fluctuations can be measured directly. At the scales lower than pc, H I structures are studied with the help of absorption measurements of the H I against background sources.

The power spectrum of the H I intensity fluctuations along the Galactic plane is measured to be  $-2.0$  to  $-3.0$  (Crovisier and Dickey, 1983). In a similar study performed by Green (1993), it was found that the power spectrum of the Galactic H I has a power-law index between  $-2.2$  to  $-3.0$ . A study of the opacity fluctuation power spectrum by Roy et al. (2010) has shown the power spectrum of the optical depth has slope  $-2.86$  for the Galactic ISM in the direction of the Cassiopeia-A. Deshpande et al. (2000) found that the H I optical depth power spectrum has a slope of  $-2.75$  for the Perseus arm towards Cassiopeia-A, whereas, they find the slope to be  $-2.5$  for the local arm toward Cygnus. Power spectra of the H I column density for 16 spiral Galaxies (taken from THINGS, see Walter et al. (2008)) have shown the power-law index in the range of  $-1.5$  to  $-1.8$  at the scales of kpc and are found to be originating from the 2D structures of H I (Dutta and Bharadwaj, 2013). In a similar study, Dutta et al. (2009) found that the power-law index has values from  $-2.5$  to  $-2.8$  at the subparsec scales. Power spectra measurement of Galactic opacity fluctuations at the au scales also has shown to have the slope of  $-2.81$  (Dutta et al., 2014; Roy et al., 2012). Such a measurement from the dust emission in the direction of the Cirrus has shown to follow a power-law with an index  $-2.9$  below 0.01 pc. These studies of the spectral

slope measurements raise two basic questions, 1) Do the singular turbulence cascade exist from the kpc to mpc scales, or 2) it is because we are mapping power spectra only in few directions in the Galaxy. To answer such a question, we identified Galactic supernovae remnants as a background source to map the optical depth power spectrum in our Galaxy in the 15 directions. As these supernovae remnants are located in the different parts of the Galaxy and are extended sources, they are suitable for our scientific purpose. The optical depth fluctuation along the direction of Cassiopeia-A is already measured, as discussed earlier in the same section.

In this chapter, we also studied the model for the scale-independent anisotropic fluctuation power spectrum that is found to scale the amplitude of the isotropic power spectrum of optical depth, but not the slope. The maximum power of anisotropy measured by Kalberla et al. (2017) and Kalberla and Kerp (2016) is  $\sim 10$ , translating to 0.5 for  $\mathcal{R}$  in our anisotropic model. This shows that the amplitude of the opacity fluctuation power spectrum also suffers from anisotropic degeneracy. But this can be lifted if the statistical nature of anisotropy is studied through observations, and it may help to understand the statistical nature of the Galactic ISM deeply. In our study, even we have taken the CNM cloud to be of three-dimensional geometry, we still have not studied the effect of the velocity channel averaging in our estimator, as discussed in Lazarian and Pogosyan (2000). The assumption of uniform line shape function breaks down if we consider the thick velocity channel analysis (VCA) (Lazarian and Pogosyan, 2004) and energetics of the CNM turbulence can be studied, but this requires extended study and is beyond the scope of this work. To summarize, the study in this chapter describes how the measurements of the optical depth autocorrelation function can be used to measure the autocorrelation function of the H I column density using the radio interferometric measurements.